Proceedings of the Institute of Acoustics

EXPERIMENTS ON THE ACTIVE CONTROL OF SOUND TRANSMISSION INTO A STIFF CYLINDER USING A PIEZOELECTRIC ACTUATOR

M. E. Johnson & S. J. Elliott

I.S.V.R. University of Southampton

1 Introduction

The objective of this work is to investigate the active control of sound transmission into an enclosed cylinder. Its motivation derives from problems experienced in the space industry where payloads may be damaged during launch by the high levels of engine noise. Passive noise reduction usually has a large weight penalty associated with it, especially at low frequencies. The active reduction of the noise transmission using piezoelectric actuators is potentially a light weight solution. Piezoelectric actuators are useful for this application because they can excite a structure without having to react against anything (they introduce strains not point forces). In this study a simple single channel feedforward control system is used to reduce the sound transmission from an external harmonic signal. This does not realistically model the stochastic noise produced by a launcher engine but will demonstrate the potential for active noise control.

2 Computer modelling

To access the feasibility of actively controlling sound transmission into an enclosed cylinder, a simple computer model was set up. Rather than providing an exact prediction of the control possible in a practical experiment, the model allowed us to investigate the interaction between the structural vibration and the acoustics. Circumstances which would facilitate good attenuations using active control could then be identified. The natural frequencies of the structural and acoustic modes were taken from an existing computer model (PROXMODE) [1]. These natural frequencies were then used in the computer model constructed for this work. This model consisted of three major components: (i) The effect of forcing (i.e. the external acoustic source and the piezoelectric actuator) on the structure. (ii) The interaction or coupling between the structural modes of vibration and the acoustic modes in the cavity and hence the prediction of the resulting acoustic field. (iii) The control system and its ability to reduce the noise levels in the cavity. The following sections will give a brief description of these three components.

2.1 The forcing of the structure

The structure is driven both by a primary acoustic field and a secondary piezoelectric actuator. We will first consider the forcing of the structure due to the external acoustic field.

To model the forcing effect of an incoming plane wave on the cylinder, a simple numerical model was constructed. The broad assumption taken, was that the acoustic field at the surface of the cylinder was unchanged by the presence of the cylinder. Although this assumption may not be realistic in some circumstances, it is a useful approximation in the context of this work. We are primarily interested in active control of acoustic transmission from *any* general external acoustic field into the cylinder. So although this model does not realistically represent the excitation due to an incoming plane wave, it will provide a reasonable primary excitation on which we can explore the possibilities of active control.

The structural modes (Figure 1) of a cylinder fitted with two stiff end plates (i.e. acting as simple supports) are given by,

$$\psi s_{mn} = sin\left(\frac{m\pi x}{L}\right) \begin{matrix} cos \\ sin \end{matrix} (n\theta) \qquad (1)$$

where ψs_{mn} is the mode shape of the mn^{th} mode with m being the axial mode number and n being circumferential mode number, L is the length of the cylinder and θ describes the angle around the cylinder.

The circumferential mode shapes are combinations of *sin* and *cos* terms. It is possible to simplify this to a single term if the excitation is known and the origin of the θ coordinate is redefined to suit. In these

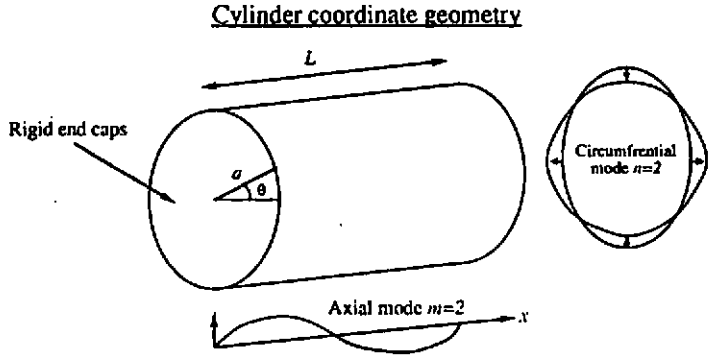

Figure 1: The cylinder used for the computer simulations. The $m = 2$, $n = 2$ mode shape is shown as an example.

simulations the modes $m = 1$ to 5 and $n = 0$ to 6 are considered. The surface of the cylinder was divided up into 20 elements along its length and 24 elements circumferentially. At any one frequency the complex pressures at each elemental position due to the incoming plane wave could be calculated. By taking the inner product of the vector of *radial displacements* due to an individual structural mode (i.e. mode shape) at the elemental positions and the vector of *pressures* at the elemental positions, a generalized forcing function for that mode could be determined.

$$f_{p_{mn}} = \psi^T_{S_{mn}}(x)p(x) \tag{2}$$

Therefore at a particular frequency, the generalized forcing function $f_{p_{mn}}$ of the mn^{th} mode is determined by the inner product of the pressures $p(x)$ at the elemental positions x and the value of the mn^{th} mode shape $\psi_{S_{mn}}$ at the elemental positions (T denotes the transpose). The absolute pressures at the elemental positions are dependent upon the amplitude of the incoming plane wave. However, our interests lie primarily with the *relative* values of the complex pressure at the surface of the cylinder and we will therefore assume some arbitrary amplitude which produces the pressures $p(x)$. We can extend this relationship to include all of the modes considered i.e.

$$f_p = \Psi^T_S p \tag{3}$$

where f_p is a vector of loading coefficients and Ψ_S is a matrix describing all of the mode shape values of the modes considered at the elemental positions. To calculate the excitation of each structural mode, the forcing functions need to be multiplied by their respective complex resonance terms. The complex resonance terms are dependent on the natural frequency of the mode considered and the frequency of excitation. These terms take into account the damping of the structure. The complex resonance term for the $(m, n)^{th}$ mode is given by,

$$a_{mn}(\omega) = \frac{\omega}{D\omega_{mn}\omega - j(\omega^2_{mn} - \omega^2)} \tag{4}$$

where D is the damping factor, a_{mn} is the complex resonance term for the mn^{th} mode when the forcing frequency is given by ω and ω_{mn} is the natural frequency of that mode. The vector a_S is a collection of these terms for the structural modes considered. From the above equation we can see that when a mode is forced at its natural frequency (i.e. $\omega = \omega_n$) the amplitude is limited by the amount of damping present.

Damping becomes less important as we move away from resonance. The excitation of the structural modes due to the forcing functions and the complex resonance terms is described by,

$$v_p = B_{fv}(f_p \odot a_S) \tag{5}$$

Where v_p is a complex vector of structural mode excitation due to the primary acoustic field, a_S is the vector of complex resonance terms for the structural modes, $\odot$ denotes a Hadamard product (i.e. an element by element multiplication) and B_{fv} is a constant which relates the forcing of the mode to the excitation. B_{fv} will be a function of the structural properties of the cylinder i.e. stiffness, density etc.

The calculation of the forcing of the structure by the piezoelectric actuator follows the approach of Lester and Lefebvre [2]. This approach models the effect of two piezoelectric ceramic patches placed on opposite sides of the cylinder walls and driven out of phase with one another. This actuator arrangement minimizes the in-plane forces (in-plane forces due to the two actuators tend to cancel) and produces a bending moment. In our experiment (section 4) only a single piezoelectric patch was used and the in-plane forces produced by the single actuator were not considered. In a more complete and accurate model these forces would have to be taken into account.

The generalized forcing functions are considered in two parts, one to dealing with the *sin* term and one to deal with the *cos* term in equation 1. The center of the piezoelectric is positioned at (x_c, θ_c) and its dimensions are defined as $(\Delta x, \Delta\theta)$. The equations which define their excitation will also be dependent on the value of n. If $n = 0$ the modal forcing functions are given by,

$$f^c_{m_0} = \frac{B_{if} m \Delta\theta}{4} sin\left(\frac{m\pi\Delta x}{2L}\right) sin\left(\frac{m\pi x_c}{L}\right)$$
$$f^s_{m_0} = 0 \tag{6}$$

$f^c_{m_0}$ is the forcing function regarding the *cos* term and $f^s_{m_0}$ relates to the *sin* term (equation 1). B_{if} is a constant which relates the input to the piezoelectric to the forcing and is a function of the piezoelectric properties of the ceramic as well as the structural properties of the ceramic, the bonding material and the cylinder. L is the length of the cylinder. If n is greater than zero then the equations are given by,

$$f^c_{mn} = G_{mn} B_{if} m \Delta\theta \left(sin\left(\frac{m\pi\Delta x}{2L}\right) sin\left(\frac{m\pi x_c}{L}\right) sin\left(\frac{n\Delta\theta}{2}\right) cos(n\theta_c)\right)$$
$$f^s_{mn} = G_{mn} B_{if} m \Delta\theta \left(sin\left(\frac{m\pi\Delta x}{2L}\right) sin\left(\frac{m\pi x_c}{L}\right) sin\left(\frac{n\Delta\theta}{2}\right) sin(n\theta_c)\right) \tag{7}$$

where G_{mn} is a weighting coefficient given by,

$$G_{mn} = \frac{m}{n} + \frac{nL^2}{m\pi^2 a^2} \tag{8}$$

where a is the radius of the cylinder. We can define a vector of forcing terms for the modes considered f_s. The amplitude of the structural modes will then be dependent upon the forcing vector and the vector of complex resonance terms.

$$v_s = B_{fv}(f_s \odot a_S) \tag{9}$$

where v_s is the vector of structural mode amplitudes due to the secondary source and B_{fv} relates the amplitude of the structural modes to a unit of modal forcing.

2.2 Radiation from structural modes into the acoustic cavity

The radiation from the vibrating cylinder into the inner cavity can be described by the coupling between the structural modes and the acoustic modes of the cylindrical cavity. The acoustic mode shapes are given by,

$$\psi_{A_{n'p_{m'}}} = J_{n'}(k_r r) cos\left(\frac{m'\pi x}{L}\right) \begin{matrix} cos \\ sin \end{matrix} (n'\theta) \tag{10}$$

where $J_{n'}$ is an n'^{th} order Bessel function and k_r is the radial wavenumber determined by the zero normal-particle wall boundary condition as solutions of the equation $J_{n'}(k_r r) = 0$ when $r = a$ the cylinder radius [3]. To calculate the coupling between a structural mode and an acoustic mode we integrate the product of their mode shapes at the cylinder wall and include a complex resonance term for the acoustic modes i.e.

$$c_{mn,n'pm'} = \int_S a_{A_{n'pm'}} \psi_{A_{n'pm'}}(x,\theta,r)\psi_{S_{mn}}(x,\theta)dS \tag{11}$$

where $c_{mn,n'pm'}$ is the coupling factor between the mn^{th} structural mode and the $n'pm'^{th}$ acoustic modes and $a_{A_{n'pm'}}$ is the complex resonance term for the acoustic modes taking the same form as that of equation 4. The coupling factors for all of the combinations of structural and acoustic modes can then be represented as a matrix of coupling factors C. The acoustic modes considered for these simulations were; $n' = 0$ to 6, $p = 0$ to 2 and $m' = 0$ to 4. The excitation of each of the acoustic modes is then given by the vectors,

$$\begin{aligned} s_p &= B_{ca} C v_p \\ s_s &= B_{ca} C v_s \end{aligned} \tag{12}$$

where s_p is a vector of complex acoustic mode amplitudes due to the primary excitation and s_s is the vector of complex acoustic mode amplitudes due to the secondary with unit excitation. B_{ca} is a constant which relates the vibration of the structure to the amplitude of the acoustic modes and is a function of the properties of the fluid i.e. density, speed of sound etc.

2.3 Minimization of Energy

The total acoustic energy in the cavity due to the primary excitation alone is given by the sum of the squares of each mode amplitude multiplied by a constant. In vector notation this is given by,

$$E_p = B_E(s_p^H s_p) \tag{13}$$

where E_p is the energy due to the primary, B_E is a constant and H denotes the Hermitian transpose (conjugated transpose). The total energy in the enclosure during control will be due to a *combination* of the primary and secondary sources' contributions. We can then manipulate the secondary source's amplitude and phase to reduce the total acoustic energy in the enclosure. The normalized complex amplitude of the single secondary source is u_s and hence the acoustic mode amplitudes due to the secondary source will be given by $s_s u_s$. The total acoustic energy when the secondary source is active (i.e. on) is given by,

$$E_T = B_E(s_p + s_s u_s)^H(s_p + s_s u_s) \tag{14}$$

where E_T is the total energy. This equation is a Hermitian quadratic in u_s and has a unique minimum value. The secondary source's complex amplitude required to minimize the total energy is given by [4],

$$u_{s_{opt}} = -(s_s^H s_p)/(s_s^H s_s) \tag{15}$$

where $u_{s_{opt}}$ is the optimal secondary source strength for minimizing the acoustic energy. The acoustic energy levels can thus be calculated with and without control to determine the amount of attenuation possible.

3 Results of computer simulations

The results shown here can only be an example of the very large number of possible permutations of source position, frequency range, structural characteristics etc. This section will therefore examine a configuration similar to the one tested experimentally.

For the results shown here the cylinder length is taken to be $0.94m$, the radius to be $0.45m$, the structural damping factor to be 0.02 and the acoustic damping factor to be 0.005. Thirty five structural modes and one hundred and five acoustic modes are considered in these simulations. The center of the piezoelectric actuator is placed at $x = 0.3m$ and $\theta = \frac{\pi}{2}$, and it is $100mm$ long (in x direction) and $45mm$ wide (circumferentially). The mechanical properties of the cylinder are only used in the calculation of the natural frequencies of the structural modes and are not necessary to calculate equation 15, if the natural frequencies are provided. The properties of the model cylinder are taken from [1] and are tabulated in Table 1. These properties correspond to the properties of the real cylinder tested experimentally (Section 4). The plane wave primary

Parameter	Value
Face Plates (CFRP, common)	
Thickness (mm)	1.0
Density (kg/m^3)E3	1.6
Elastic mod. (N/m^2)E9	
Tensile axial	26.2
Tensile circumf.	69.5
Shear in plane	19.3
Core (aluminium honeycomb)	
Thickness (mm)	5
Density (kg/m^3)	48
Shear mod.(N/m^2)E6	
Axial	240
Circumf.	150
Wall	
Length (m)	0.94
Diameter (m)	0.9
Mass/area (kg/m^3)	4.0

Table 1: Properties and dimensions of cylinder B used in the active control experiments.

field is incident on the cylinder at $\phi = 45^0$ to the x axis and at and angle $\theta = 0$ (Figure 1). The acoustic energy levels before and after control are shown in Figure 2. These results show that the control system has the ability in most cases to reduce the acoustic energy due to resonant behaviour. At resonance the response is dominated by a single structural and/or acoustic mode and a single channel system which can couple into this mode will in general be able to achieve good attenuations. What is more interesting are the cases where off-resonant control is achieved. This occurs in two regions in the frequency range considered; (i) $350 - 500Hz$ and (ii) $550 - 700Hz$. It is characteristic that the off-resonant response of a system will involve more than one mode. Therefore a single channel control system will generally be unable to achieve good attenuations off-resonance. However, the response of the system we are considering is due to the interaction of two sets of modes, and although the acoustic off-resonant behavior may be due to a number of *acoustic* modes they may all be excited to the largest extent by a *single structural mode*. The reduction of this structural mode amplitude will therefore produce good off-resonant attenuation. This scenario could equally occur with a single acoustic mode being excited by a number of structural modes. In this case the actuator could minimize the *net* contribution to that acoustic mode to achieve good off-resonant control.

In the case we are considering there are a number of structural *and* acoustic resonances present in the $350 - 500Hz$ frequency range. What it is important to consider is the *coupling* between the structural and acoustic modes. A single structural mode will not couple into the *majority* of the acoustic modes because they are not matched geometrically and it is therefore possible for numerous structural resonances and acoustic resonances to occur within a frequency range, and the coupling to be dominated by the interaction

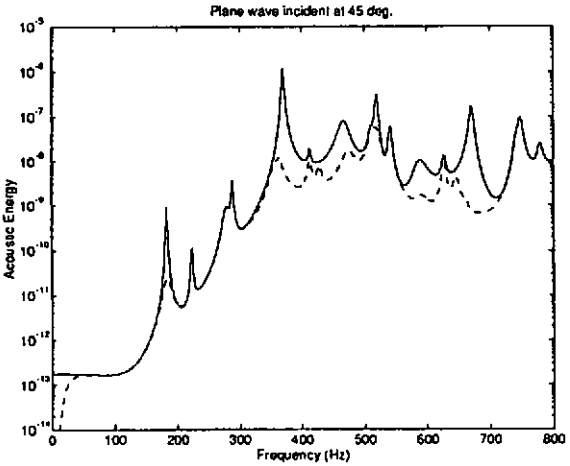

Figure 2: The acoustic energy present in the cylindrical cavity before (solid) and after control (dashed) when controlling the transmission due to an incoming plane wave incident at 45^0.

of a single structural mode with a single acoustic mode. It so happens that in this simulation the $n = 2$, $m = 1$ structural resonance ($467Hz$) has a natural frequency close to the $n' = 2$, $p = 0$, $m' = 0$ acoustic mode ($370Hz$). These two modes couple very well geometrically , and most of the other structural and acoustic modes in this frequency range do not couple at all. It is therefore possible amongst a large number of individual resonances to still achieve good off-resonant attenuation using a single channel control system. Similarly the control in the $550 - 700Hz$ range seems to be due to good geometric coupling between the $n = 4$, $m = 2$ structural mode ($586Hz$) and the $n' = 4$, $p = 0$, $m' = 1$ acoustic mode ($671Hz$).

4 Experiment

The experimentation was carried out on a model cylinder, which was originally constructed as a 1/6 scale model of an Ariane 5 fairing [1]. The cylinder was of dimension $L = 0.94m$ and $a = 0.45m$ (Figure 3.) and constructed of thin aluminium honeycomb covered by carbon fibre re-enforced plastic. The end caps were made of $8mm$ steel to provide stiff (simply supported) end conditions. The cylinder was suspended from the ceiling of a large anechoic chamber by steel cables connected to the end caps. The primary sound field for the experiment was generated by an 8 inch loudspeaker. The secondary actuator used was a large ($100mm \times 45mm \times 2mm$) piezoelectric ceramic which was driven via a 1 to 128 Quad step-up transformer (used for electrostatic loudspeakers) to produce high drive voltages from low voltage amplifiers. The actuator can be driven with voltages of over $1000V$ but for our purposes it was only necessary to use between 50 and 200 volts. The piezoelectric ceramic was fixed to the cylinder using epoxy glue and this involved the gluing of the flat piezoelectric surface to the curved cylinder. An epoxy base was therefore required to produce a flat surface to which the actuator could be glued. This is probably undesirable for high excitation levels. In a real implementation however, bases could be made of stiffer material (i.e. metal) or the actuators themselves could be curved. It may also be possible to integrate the actuators into the face plate construction of the fairing sandwich wall. To observe the sound pressure inside the cavity, five electret microphones were used

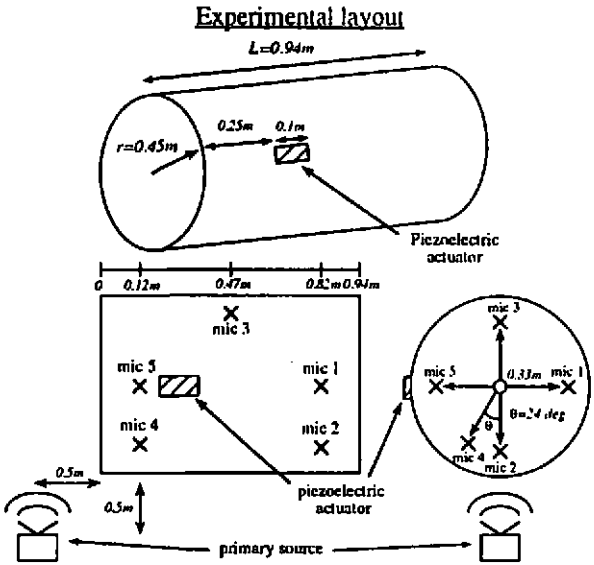

Figure 3: The experimental layout of the cylinder showing the microphone locations, the secondary actuator's position and the two primary source positions.

and placed in the positions shown in Figure 3. A single accelerometer was placed a various points on the external structure to measure the vibration levels present and to determine the dominant structural mode present at various frequencies.

4.1 Broadband frequency response measurements

The frequency responses between the input to the primary source and the five microphones and the frequency responses between the input to the secondary source and the five microphones was measured over the $0-800Hz$ frequency range. If the frequency responses between the primary source and the microphones are known, the best attenuations possible can be calculated over a range of frequencies. The frequency responses between the loudspeaker and the five microphones (at a single frequency), can be described by a five element complex vector $\boldsymbol{T}_p$ and similarly for the secondary actuator as $\boldsymbol{T}_s$. The sum of the mean squared pressures at the microphone positions can then be calculated for any combination of source strengths as,

$$P_T = (\boldsymbol{T}_p + \boldsymbol{T}_s u_s)^H (\boldsymbol{T}_p + \boldsymbol{T}_s u_s) \tag{16}$$

where P_T is the sum of the mean squared pressures at the microphone positions and u_s is the source strength of the secondary source and the primary source is assumed to have unit amplitude. This equation is very similar to equation 14 which describes the acoustic energy in the cylinder and there is a unique secondary source strength $u_{s_{opt}}$ which minimizes this function. This is given by,

$$u_{s_{opt}} = -\frac{\boldsymbol{T}_s^H \boldsymbol{T}_p}{\boldsymbol{T}_s^H \boldsymbol{T}_s} \tag{17}$$

By substituting the optimal secondary source strength back into the equation for the sum of the squared pressures (equation 16) and dividing by the original pressure (i.e. before control) we can calculate the ratio

of the sum of the squared pressures before and after control,

$$\frac{P_{T_{opt}}}{P_{T_p}} = 1 - \frac{\mathbf{T}_p^{H}\mathbf{T}_s\mathbf{T}_s^{H}\mathbf{T}_p}{\mathbf{T}_s^{H}\mathbf{T}_s\mathbf{T}_p^{H}\mathbf{T}_p} \tag{18}$$

The sum of the mean squared pressures $P_{T_{opt}}$ is obtained when the secondary source strength is set to the optimal value and the sum of the mean squared pressures when $u_s = 0$ is given by $P_{T_p} = \mathbf{T}_p^{H}\mathbf{T}_p$. The frequency response of the secondary source itself will effect the frequency responses between the input to the secondary source and the outputs of the microphones in the same way and will cancel in equation 18. The important factor will be the relative differences in the frequency responses of the *paths* between the secondary source and the five microphones. Similarly, the primary source's frequency response (i.e. the frequency response of the electronics, the loudspeaker and its radiation efficiency) will not affect the estimates of attenuation. This will however affect the values of the sum of the squared pressures (i.e. $P_{T_{opt}}$ and P_{T_p}) observed. These values are also affected by the microphones' frequency responses and we must assume that their responses are all flat or at least similar to each other.

4.2 Attenuation prediction

The frequency responses between the primary source and five microphones, is used to produce the solid line graph in Figure 4, which represents the sum of the squared pressures measured at the microphone positions due to the primary source alone. The dashed line represents the sum of the squared pressures at the microphone positions after control (Equation 18). This graph displays many sharp resonances across

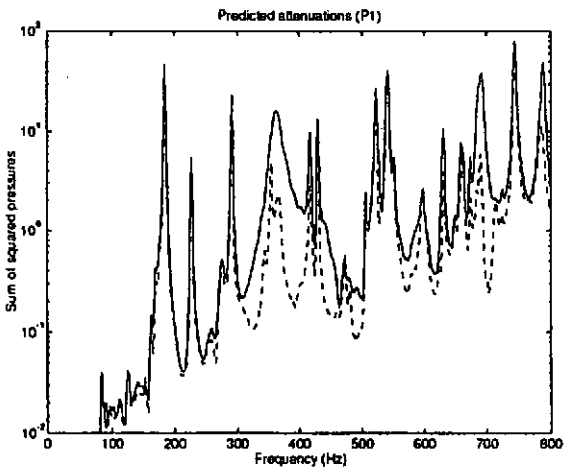

Figure 4: The sum of the 5 squared pressures measured at the microphone positions without control (solid) and the levels predicted after control (dashed) for the primary source.

the frequency range which all seem to be attenuated to some extent by the control system (between $2-5dB$). There are also two regions of significant off resonant control, the first being between $300-450Hz$ and the second between $670-720Hz$. This corresponds well to the regions of attenuation predicted by the computer model in section 3.

4.3 Single channel control

The frequency response measurements (section 4.1) allow us to predict what attenuations our control system would achieve over a range of frequencies. To ensure that these predictions are valid, experiments were carried out at two frequencies in the frequency range considered ($359Hz$ and $415Hz$ i.e. $60Hz$ and $69Hz$ full scale). The control was carried out manually by altering the phase and amplitude of the input to the secondary source while monitoring the response of the microphones. Although this adaption method is crude the results can be directly compared with the predictions above at single frequencies and may give us some confidence in the results of the frequency response measurements to predict the attenuations accurately.

The resulting reductions in mean squared pressure levels at the microphone positions were $10dB$ and $7dB$ respectively. This corresponded very well to the $10.6dB$ and $5.3dB$ attenuations predicted by the frequency response measurements at these frequencies. These values of attenuation are taken from the data displayed in Figure 4. A slightly larger reduction was measured than predicted at the higher excitation frequency. This is probably because the excitation frequency was not very accurately measured in the active control experiment and the predicted reductions in Figure 4 are very frequency dependent.

4.4 Accelerometer results

The frequency responses between the sources and an accelerometer placed on the cylinder was measured for various accelerometer locations (Figure 5). These measurements allowed us to observe the structural

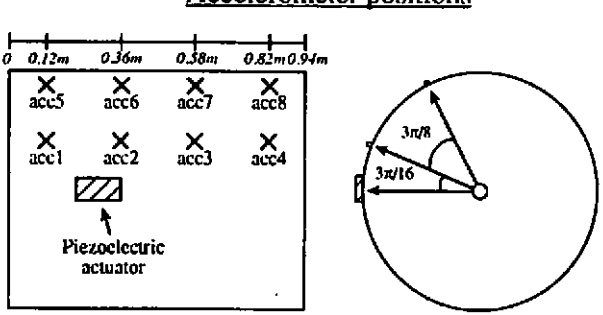

Figure 5: The eight accelerometer positions on the cylinder.

resonances and compare their natural frequencies with those predicted from the computer simulation. The mode order was deduced from the shape of the measured axial acceleration and the relative phases of the acceleration circumferentially. This was sufficient to identify the first few modes. Figure 6 shows the frequency response between the input to the piezoelectric actuator and the accelerometer at position 1. The observed natural frequencies of the first few modes fall within 4 percent of the predicted natural frequencies (Table 2). The measured response often had double peaks (probably due to asymmetries within the cylinder) and therefore both peak frequencies are quoted. At any given frequency, the relative phases of the frequency responses at the different accelerometer positions allow us to confirm that the mode observed is the one predicted to be dominant at that frequency.

5 Conclusions

This work demonstrates that although precise modelling of every feature of sound transmission into a cylinder

Mode (m,n)	Predicted	Measured
(1,4)	268	259
(1,5)	353	345 or 353
(1,2)	467	461
(2,5)	535	522 or 531

Table 2: Predicted and measured natural frequencies of the first few structural modes in Hz.

cannot be represented using a simple theoretical method, the important physical aspects which determine the overall performance of an active control system can be represented. For the cylinder considered it was generally the interaction between specific structural and acoustic modes which determine the performance. It has also been demonstrated that these potential reductions can be achieved in practice for a pure tone primary excitation.

Given that much of the sound transmission in a frequency range could be due to a single structural mode, a modal sensor designed to sense that mode could be used in a feedback control system to reduce the sound transmission in that frequency range, regardless of the primary source type (i.e. random or deterministic).

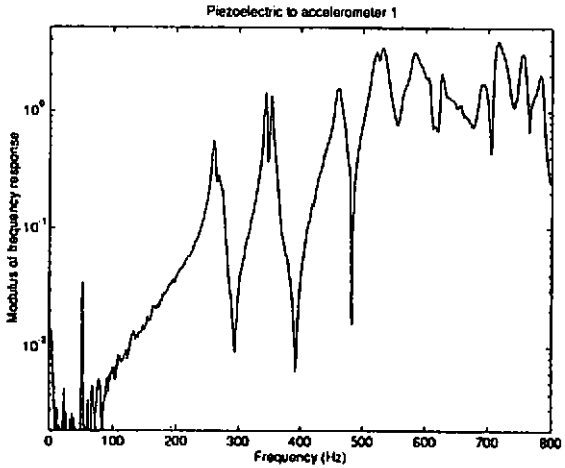

Figure 6: The frequency response of accelerometer 1 to the piezoelectric actuator.

References

[1] J. N. Pinder, M. E. House and F. J. Fahy. 1987. Final report, ESA Contract No 6675/86/F/FL *A Preliminary Study of the Ariane 5 Payload Bay Given by the Fairing and SPELTRA*

[2] H. C. Lester and S. Lefebvre 1993. Journal of Intelligent Material Systems and Structures. Vol. 4 Pg. 295-306 *Piezoelectric Actuator Models for Active Sound and Vibration Control of Cylinders*

[3] F. Fahy. Academic Press 1985 Pg 205-210 *Sound and Structural Vibration*

[4] P. A. Nelson and S. J. Elliott Academic Press 1992 *Active Control of Sound*